Optimizing Oxygen Functional Groups on Porous Carbon Monoliths by Green Activation Promotes Seawater Hydrogen Evolution

Bei Li[a], Shiyang Fei[b*], Zhenlu Liu[a], Changshui Wang[a], Zhiqiang Sun[a], Chunmei Zhang[c*], Haoqi Yang[d], Hongliang Zhao[e], Qian Zhang[a, f*], Shuijian He[a*]

[a] Co-Innovation Center of Efficient Processing and Utilization of Forest Resources, International Innovation Center for Forest Chemicals and Materials, Nanjing Forestry University, Nanjing 210037, China

[b] Guangdong YounYan Energy Technology Co., Ltd, Guangzhou 510515, China

[c] Institute of Materials Science and Devices, School of Materials Science and Engineering, Suzhou University of Science and Technology, Suzhou 2150009, China

[d] Institute of Technology for Carbon Neutralization, College of Electrical, Energy and Power Engineering, Yangzhou University, Yangzhou, Jiangsu 225127, China

[e] Key Laboratory of Quality Safe Evaluation and Research of Degradable Material, State Administration for Market Regulation; Hainan Academy of Inspection and Testing, Haikou, Hainan 570203, China

[f] Fujian Key Laboratory of Eco-Industrial Green Technology, College of Ecology and Resources Engineering, Wuyi University, Wuyishan 354300, China

E-mail: camazfei@163.com (Shiyang Fei), cmzhang@usts.edu.cn (Chunmei Zhang), zhangqian5689@njfu.edu.cn (Qian Zhang), shuijianhe@njfu.edu.cn (Shuijian He)

Experimental Section

Materials and Chemicals: Potassium hydroxide (KOH), sodium chloride (NaCl), and hydrogen peroxide (H_2O_2, 30%) were purchased from Sinopharm Co. Ltd and used without further purification. Natural seawater was obtained from Qingdao, China. Natural poplar wood was sourced by Chenlin Industrial Co. Ltd.

Fabrication of CW: Natural poplar wood was cut into small cross-section chips with dimensions of 2 × 2 × 0.2 cm^3 (length × width × height). The wood chips were then subjected to thermal treatment in a tube furnace. Initially, the chips were heated at 260 °C for 2 hours, followed by further and then heated at 1000 °C for 2 hours under an N_2 atmosphere to produce carbonized wood (CW). The CW was subsequently modified by reacting it with H_2O_2 in a reaction vessel containing 60 mL of 1 wt% H_2O_2 solution. The reaction vessel was heated in an oven for 1, 3, and 5 hours.

Characterization: Electrochemical measurements were performed using a CHI 760E electrochemical workstation. The surface morphologies of the samples were characterized with a Hitachi SU8010 field emission scanning electron microscope (FESEM). Phase and chemical composition analyses were performed using X-ray diffraction (XRD, Ultima IV) and X-ray photoelectron spectroscopy (XPS, ESCALAB 250XI). Raman spectra were recorded with a DXR532 Raman spectrometer with a 532 nm laser. Nitrogen adsorption-desorption isotherms were measured using a Quantachrome Autosorb IQ to determine the Brunauer-Emmett-Teller (BET) specific surface area. Water contact angles were measured with a JC2000 device.

Electrochemical Measurements: All measured potentials were referenced to a reversible hydrogen electrode (RHE) using the Nernst equation ($E_{RHE} = E_{Hg/HgO} + 0.059 \times pH + 0.098$ V). The linear sweep voltammetry (LSV) measurements were carried out at a scan rate of 1 mV s^{-1} with an automatic 95% compensation on an electrochemical workstation. Nyquist plots were obtained over a frequency range of 0.1 Hz to 100 kHz

with an amplitude of 5 mV. Catalyst durability was assessed using the chronoamperometry method.

DFT calculations

The spin-polarized density functional theory (DFT) calculations were performed using the Vienna Ab-initio Simulation Package (VASP) [1-2], which incorporates Projected Augmented Wave (PAW) pseudopotentials [3]. The exchange-correlation energy was treated using the generalized gradient approximation (GGA) method with the Perdew-Burke-Ernzerhof (PBE) functional [4-5]. A plane-wave energy cutoff of 450 eV was employed. The Monkhorst-Pack scheme with a k-point mesh of 3 × 3 × 1 and a k-point spacing of 0.05 $Å^{-1}$ was used to sample the first Brillouin zone [6]. All atoms were fully relaxed during the optimizations. A vacuum space of 15 Å was applied above the molecular system to prevent periodic interactions throughout the calculations. Geometry relaxation was carried out using the Quasi-Newton l-BFGS method until the maximum energy and force on each degree of freedom were less than 1.0×10^{-5} eV and 0.01 eV/Å, respectively.

To obtain the free energy profile, Gibbs free energies for all states were calculated based on the ZPE-corrected DFT total energy, set as the enthalpy at 0 K. The free energy was calculated using the following expression:

$$G = H - TS = E_{DFT} + E_{ZPE} + \int_{0}^{298.15K} C_V dT - TS$$

where E_{DFT} is the total energy from DFT optimization, E_{ZPE} is the zero-point vibrational energy, C_V is the heat capacity, T is the temperature in Kelvin, and S is the entropy. The free energy for the gas-phase molecule was calculated using standard thermodynamic data at the standard state (refer to www.nist.com).

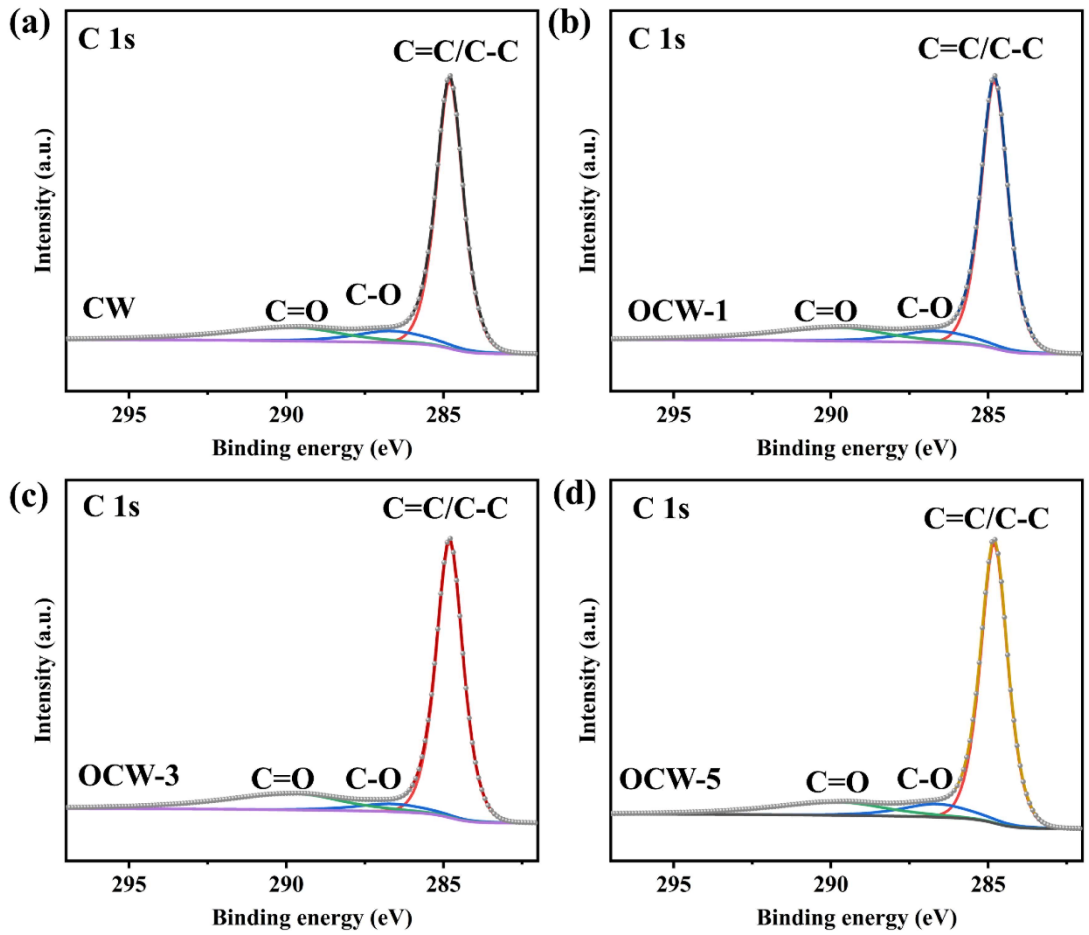

Fig. S1 High-resolution C 1s spectrum of CW (a), OCW-1 (b), OCW-3 (c), OCW-5 (d).

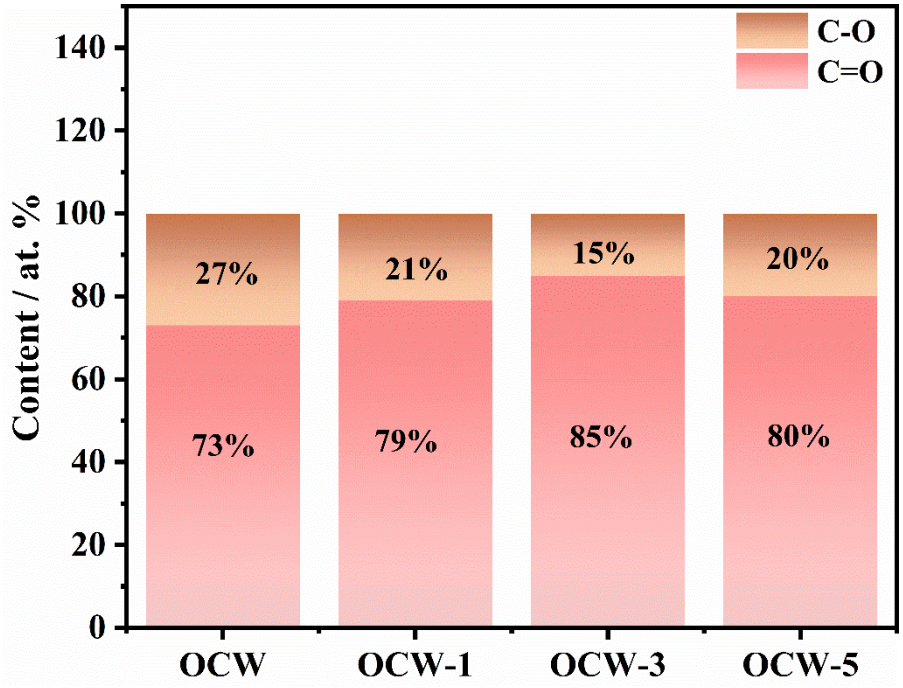

Fig. S2 The proportion of oxygen-containing functional groups in different samples.

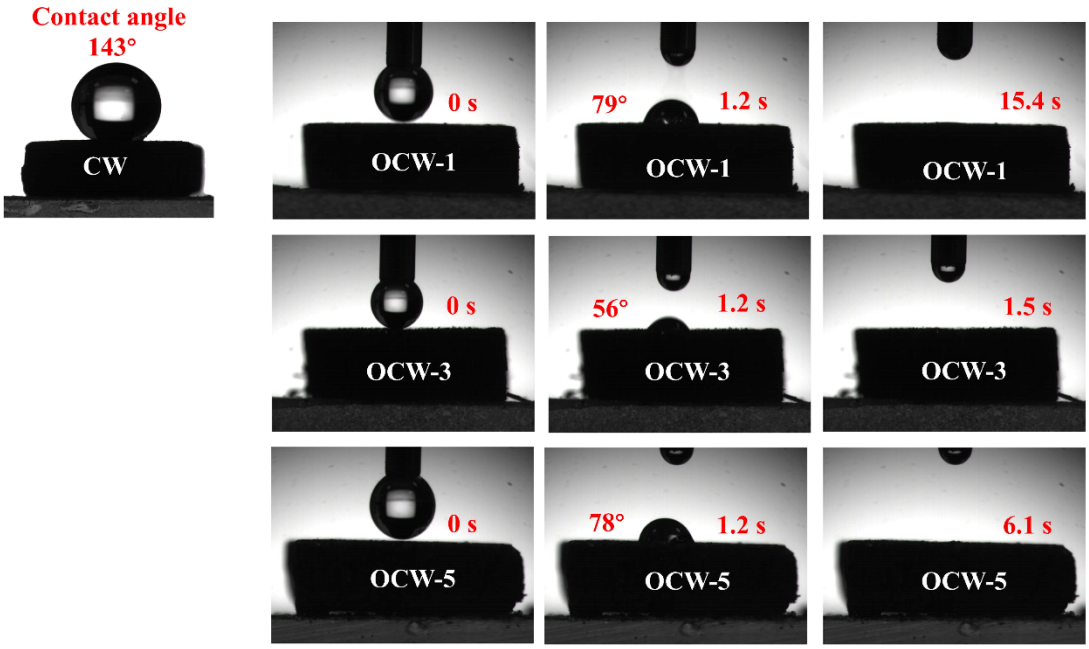

Fig. S3 Water contact angle measurements of CW, OCW-1, OCW-3, and OCW-5.

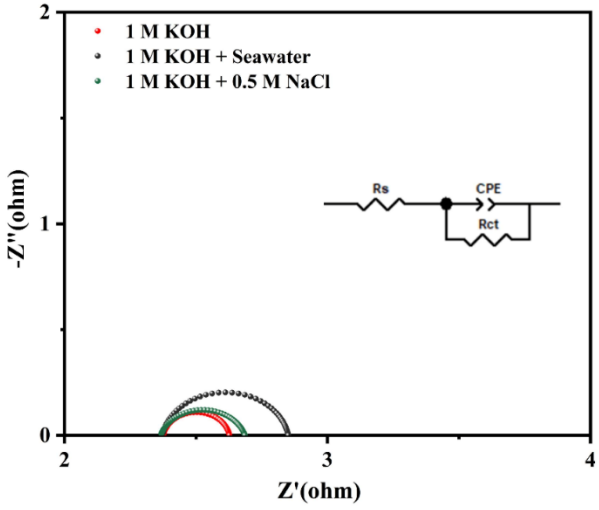

Fig. S4 EIS plots of OCW-3 in different electrolytes.

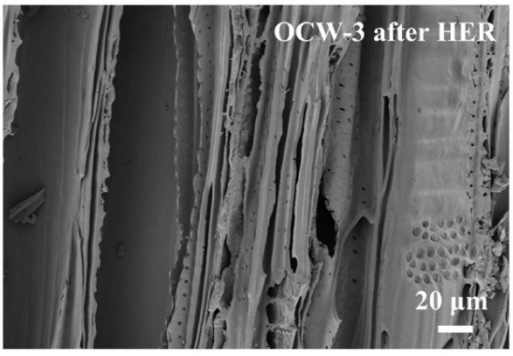

Fig. S5 SEM images of OCW-3 after HER.

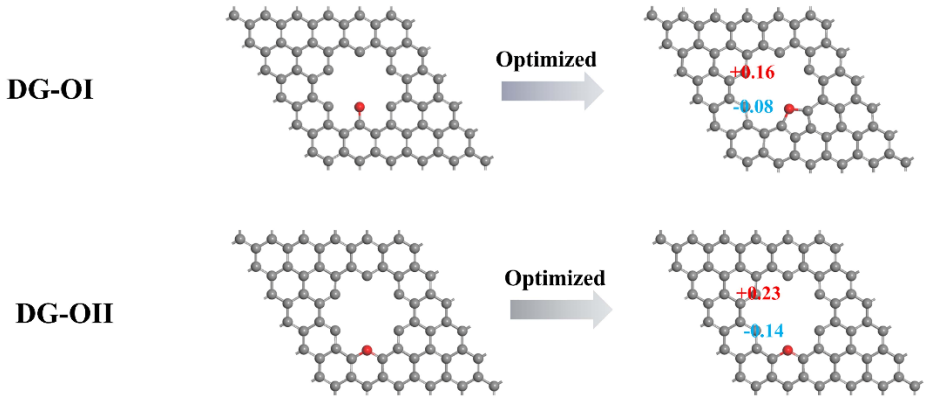

Fig. S6 Optimized model structure of DG-OI and DG-OII.

Fig. S7 The structures of G, DG, DG-OI and DG-OII in the electrocatalytic alkaline hydrogen evolution process.

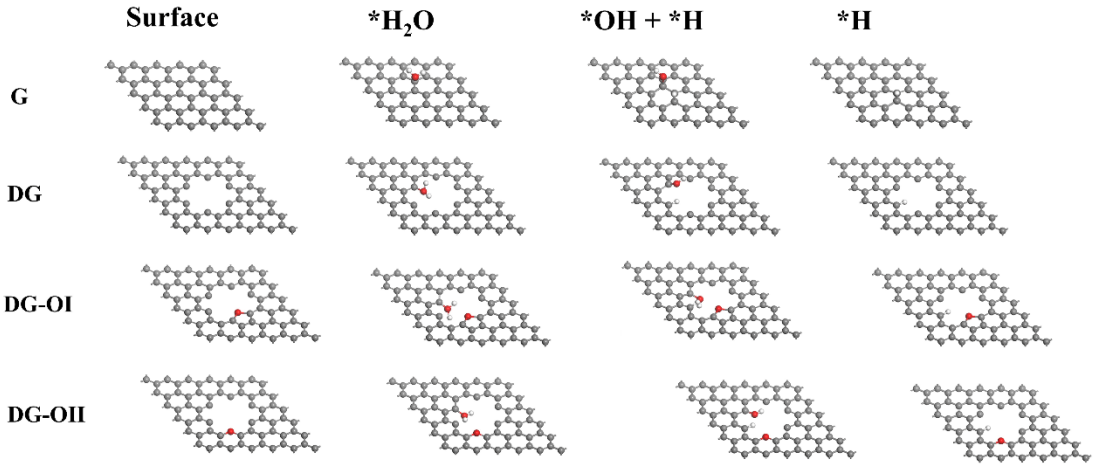

Table S1 The content of different oxygen-containing functional groups in CW, OCW-1, OCW-3, and OCW-5 before the HER test and OCW-3 after the HER test.

Samples	O-I (C=O)	O-II (C-O)
CW	3.97 At. %	1.47 At. %
OCW-1	5.00 At. %	1.27 At. %
OCW-3	5.48 At. %	0.99 At. %
OCW-5	4.98 At. %	1.20 At. %

Table S2 Comparison of HER performance of different carbon-based catalysts.

Carbon sources	**η_{10} (mV)**	**Tafel slope (mV dec^{-1})**	**Electrolytes**	**Ref.**
Silk cocoon	354	310	1 M KOH	7
Luffa sponge	492	253	0.5 M H_2SO_4	8
Catkin	741	179	1 M KOH	9
Catkin (NiOOH@C-MC)	696	180	1 M KOH	9
Catkin (MoS_2@C-MC)	523	223	1 M KOH	9
Cypress leaves	253	286	1 M KOH	10
Cattail spike (NBCF)	363	550	1 M KOH	11
Wood	245	171	1 M KOH	This work

References

1. G. Kresse, J. Hafner, *Phys. Rev. B,*1993, **47**, 558-561.

2. G. Kresse, J. Hafner, *Phys. Rev. B,* 1994*,* **49**, 14251-14269.

3. P. E. Blöchl, *Phys. Rev. B,* 1994, **50**, 17953-17979.

4. G. Kresse, D. Joubert, *Phys. Rev. B,* 1999, **59**, 1758-1775.

5. J. P. Perdew, K. Burke, M. Ernzerhof, *Phys. Rev. Lett.,* 1996, **77**, 3865-3868.

6. Monkhorst, H.J. and J.D. Pack, Physical Review B, 1976, **13**, 5188-5192.

7. W. Xiao, Y. Li, Y. Zhang, P. Wang and N. Qi, *Fuel*, 2024, **369**, 131797.

8. C. R. Ratwani, S. Karunarathne, A. R. Kamali and A. M. Abdelkader, *ACS Appl. Mater. Interfaces*, 2024, **16**, 5847-5856.
9. J. Liu, S. Zhao, C. Wang, Y. Ma, L. He, B. Liu and Z. Zhang, *J. Colloid Interface Sci.*, 2022, **608**, 1627-1637.
10. M. Krishnamachari, P. Vijayakumar, M. Kumar, M. Senthil Pandian and J.-H. Chang, *Mater. Lett.*, 2024, **357**, 135652.
11. S. Hong, N. Song, E. Jiang, J. Sun, G. Chen, C. Li, Y. Liu and H. Dong, *J. Colloid Interface Sci.*, 2022, **608**, 1441-1448.